Photoelectrochemical degradation of lignin

R. PELEGRINI[1], J. REYES[1], N. DURÁN[1], P.P. ZAMORA[2] and A.R. DE ANDRADE[3]*
[1]*Universidade Estadual de Campinas, Instituto de Química, C.P. 6154, CEP: 13083-970, Campinas-SP, Brazil*
[2]*Universidade Federal do Paraná, Departamento de Química, Curitiba-PR, Brazil*
[3]*Departamento de Química da FFCLRP-USP, Av. Bandeirantes 3900, 14040-901, Ribeirão Preto-SP, Brazil*
(*author for correspondence*)

Abstract

We have evaluated the efficient of degradation of lignin by an photoelectrochemical process. Using a Ti/$Ru_{0.1}Sn_{0.6}Ti_{0.3}O_2$ electrode, a quartz reaction device and an artificial ultraviolet light, decoloration ratios higher than 70%, and reductions of 51% and 83% in TOC and total phenol products, respectively, were observed for a reaction time of 6 h. Comparing these values with the sum of the decoloration ratios (or TOC and total phenol reductions) obtained by separate measuring of electrochemical and photochemical procedures, a significant synergetic effect between these two processes was observed. Furthermore, the degradation capacity of the photoelectrochemical process increases as the SnO_2 content is increased.

1. Introduction

The paper industry faces considerable environmental problems associated with pulp manufacture, in which a large number of persistent and toxic chemicals are produced [1, 2]. In the wood pulping process by the Kraft process, the wood chips are submitted to an alkaline process in the presence of sodium sulphide results in the elimination of about 95% of the lignin content. The black liqueur which is generated contains several polyphenolic species derived from lignin fragmentation. In the subsequent pulp bleaching processes the remaining lignin (∼5%) is eliminated with chlorine and chlorine dioxide. Consequently, many chlorinated organic compounds of high and low molecular weight (generically denominated chlorolignins and chlorophenols) are generated at this stage, including the highly toxic dioxins and furans [3, 4]. For this reason, the detection of chlorinated organic compounds in marine sediments from regions located near paper industries is frequently observed [5].

Due to the relatively low efficiency of the biological processes used in the remediation of these effluents [1], much effort has been dedicated to the minimisation of toxicity. Many of these studies have been directed towards the substitution of chlorine chemicals, as a way to eliminate the adsorbable organohalide compounds (AOX). With the establishment of the elemental chlorine free (ECF) and totally chlorine free (TCF) processes, the AOX levels were greatly reduced or completely eliminated from the effluents. Unfortunately, even with these modifications the toxicity remains very high, due to the presence of compounds which have as yet not been identified [6]. Therefore, the discharge of toxic effluents generated by the paper industry remains a critical problem.

The efficiency of heterogeneous photocatalytical processes in the degradation of recalcitrant chemical compounds using titanium dioxide has been extensively documented [7–11]. However, the difficulties associated with the separation of the semiconductor after the photochemical treatment [12] together with inactivation of the photocatalyst by recombination of the photogenerated electron-hole pair [1] have impeded the implementation of a continuous photochemical effluent treatment system. Alternatively, a wide range of electrochemical processes have been proposed for the degradation of toxic residues [13, 14]. Although attractive due its operational simplicity [15], the degradation yield of lignin by electrochemical methods is still very low [16]. In early work, a TiO_2 anode was proposed for photoelectrochemical decomposition of water [17]. Subsequently, several photoelectrochemical procedures have been proposed for the degradation of chemical pollutants [18, 19].

In this paper we report for the first time the use of DSA® in the degradation of a lignin-sulphonate compound, using an electrochemically assisted photocatalytic process. A ternary oxide electrode composition was chosen, since as previously reported [20], the electrochemical mechanism is closely related to the electrode composition. A mixture containing low amounts of

active oxide (RuO_2) and rich in a *nonactive* oxide (SnO_2) was chosen. An electrode composed of an *active* oxide promotes the oxygen evolution reaction (OER) which is simultaneous with organic oxidation (RuO_2) where a *nonactive* oxide (SnO_2) promotes organic oxidation via hydroxyl radical formation. TiO_2 when introduced into the mixture not only catalyses the degradation of lignin in the photochemical reaction but also promotes mechanical stability. Three different electrode compositions were investigated: $Ti/Ru_{0.1}Ti_{0.9}O_2$; $Ti/Ru_{0.1}Sn_{0.2}Ti_{0.7}O_2$ and $Ti/Ru_{0.1}Sn_{0.6}Ti_{0.3}O_2$.

The advantages of the photoelectrochemical process using DSA® electrodes can be summarized as follows: (i) the use of a ternary oxide mixture can modulate the electrochemical and photochemical properties of the electrode and also permits reduction of the electrode production cost; (ii) the use of oxide coatings overcomes the problems associated with the elimination of homogeneous semiconductors at the end of the process; (iii) from a photochemical aspect, the application of an external potential permits electron collection at the semiconductor coating, which inhibits the recombination process of the electron-hole pair [21]; (iv) the photoactivation of highly reactive chemical species formed on the electrode surface, such as O_3, $OH^\bullet$ and H_2O_2, significantly enhances the degradative capacity of the combined electrochemical and photochemical processes.

2. Experimental details

Titanium plates were purchased from Ti-Brasil Titânio Ltda (Brazil). Lignin-sulphonate was supplied by Vixil SPC Melbar and was used as received. The concentration of lignin-sulphonate (LS) in the photoelectrochemical experiments was 2000 mg L^{-1}. Ruthenium, titanium and tin chlorides (Aldrich) were used without any further purification. Stock solutions composed of 0.2 mol dm^{-3} $TiCl_4$, 0.2 mol dm^{-3} $RuCl_3.2H_2O$ and 1.25 mol dm^{-3} $SnCl_2.2H_2O$, were prepared in 1:1 (v/v) HCl. Ruthenium and titanium chloride solutions were gravimetrically standardised while $SnCl_2$ was standardised by atomic absorption spectrophotometry (Perkin–Elmer 5000 atomic absorption spectrophotometer), using an N_2O-acetylene flame. Mixed oxide layers were prepared by thermal decomposition (400 °C) of the stock solutions, which were mixed according to the desired oxide coatings ($Ti/Ru_{0.1}Ti_{0.9}O_2$; $Ti/Ru_{0.1}Sn_{0.2}Ti_{0.7}O_2$ and $Ti/Ru_{0.1}Sn_{0.6}Ti_{0.3}O_2$). Pretreatment of the titanium support and the electrode deposition were carried out according to the method described by Boodts and Trasatti [22]. The final coating (2 μm) was annealed under an oxygen flux (5 L min^{-1}) for 4 h.

X-ray diffractograms were carried out in a Carl Zeiss URD-6 diffractometer (CuK_α, 30 kV, 20 mA, 0.1°/3s). SEM micrographies were obtained with a Jeol T-300 scanning electron microscope, using a 20 keV electron beam. In order to avoid metal base interference the experimental EDX measurements were optimised so that the penetration depth of the beam was minimal.

Electrochemical measurements were carried out using an EG&G PAR model 273-A potentiostat using a standard three-compartment cell with a Pt wire gauze counter electrode and a saturated calomel electrode (SCE) as reference.

The gel permeation chromatographic (GPC) analyses were carried out in a Waters 510 liquid chromatography apparatus, using a Ultrahydrogel column (7.8 × 300 mm) and water as a mobile phase.

The photoelectrochemical treatments were carried out in a single compartment cell coupled to dual collimated light beams provided by 250 W high-pressure mercury vapour lamps (Figure 1). These ultraviolet sources provide an intense emission band centred at 254 nm. As shown in Figure 1, the working electrode (20 mm × 25 mm × 0.9 mm) was centred in the cell between two cathode grids (titanium grid of 15 mm × 25 mm × 1.0 mm) located on either side the anode at a distance of 3 mm. The distance between the lamps and the quartz reactor wall was 6.0 cm. The process was maintained at 35 °C by air refrigeration of the photoelectrochemical apparatus, and a thermometer was placed inside the cell to monitor the temperature during the experiments. The voltage across the working and the counter electrode pair was kept constant at 2.0 or 6.0 V by an external power supply (Hewlett Packard 6255A). The potentials were held at the oxygen evolution reaction (OER), and under these conditions the observed current was constant around 60 and 95 mA, respectively.

All the experiments were performed in an unbuffered aqueous medium and the initial pH of the lignin sulphonate solution was 11. On completion of the photoelectrochemical degradation process, the pH of the solution dropped to 9.5 due to the conversion of adsorbed hydroxyl ions to hydroxyl radicals at the TiO_2 surface ($TiO_2 + H_2O + h^+ \rightarrow Ti(OH^\bullet) + H^+$). As reported previously for many organic compounds [23] the formation of acid species from partial lignin degradation cannot be discounted.

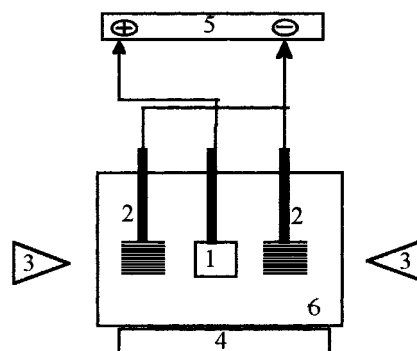*Fig. 1.* Electrochemical assisted photochemical reactor. (1) $Ti/Ru_{0.1}Sn_{(0.1-x)}Ti_xO_2$ electrode, (2) titanium grid (cathode), (3) 250 W mercury lamp, (4) magnetic stirrer, (5) d.c. source, (6) quartz reaction device.

The experiments were conducted under alkaline conditions (pH 11) since paper industry wastewaters are recovered in basic medium, and furthermore the OER is displaced a few hundred millivolts in alkaline medium as compared to an acid medium [24]. This gain in the overpotential is critical in determining the energetic cost of the whole process. No supporting electrolyte was added since the main goal was to simulate conditions of wastewater recovery produced by the paper industry.

The efficiency of the oxidation process was evaluated by monitoring three parameters: the decolorization ratio (defined as the ratio between the initial and final absorbance measurement at 465 nm (A_{465}) at pH 7.6) in a Hitachi U-2000 spectrophotometer; the reduction of the total organic carbon content in a TOC-5000 Shimadzu Total Organic Analyser; and the reduction of total phenolic content by Folin–Ciocalteu's reaction using colorimetric methodology (Apha, 1989).

3. Results and discussion

3.1. SEM and EDX characterization of the working electrode

A scanning electron micrograph of the Ti/$Ru_{0.1}Sn_{0.2}Ti_{0.7}O_2$ electrode is shown in Figure 2 in which the characteristic 'cracked-mud' morphology with large grains and cracks is observed. The SEM analysis of the electrode surfaces is very similar to those reported in the literature for Ti/$Ru_{0.2}Sn_xTi_{(0.8-x)}O_2$ electrodes [25], showing that, even for a low content of the electrochemically active oxide (RuO_2), the 'cracked-mud' morphology is maintained. After the electrochemical treatment no significant changes were observed, demonstrating that the electrode is quite stable under the experimental conditions used.

The EDX analysis, measured on several areas of the oxide surface, showed only rutilic TiO_2 formed by thermal decomposition during fabrication of the electrode (400 °C, 4 h calcination and O_2 flux). Similar results have been observed by many authors [26]. Although the more photoactive TiO_2-anatase form was not observed, by mixing SnO_2 and TiO_2 in
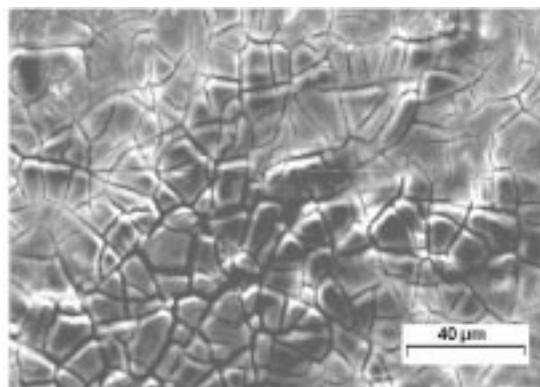

Fig. 2. SEM micrography of Ti/$Ru_{0.1}Sn_{0.6}Ti_{0.3}O_2$ electrode.

appropriate amounts, the energy gap limitation for photoexcitation may be overcome to achieve efficient charge separation which permits LS degradation. Therefore SnO_2 can act as a sink for the photogenerated electrons, lowering the band gap-separation [21, 27]. Figure 3 shows the photochemical charge separation for this system.

3.2. Electrochemical analysis

The electrochemical characterization of the electrode surface was performed in a 1.0 mol dm^{-3} HClO$_4$ solution. The normal $I \times E$ pattern was observed in the voltamograms for all anode compositions used in this study. This pattern is characterized by broad peaks and is very similar to those reported previously [22, 28].

Figure 4 shows the cyclic voltammogram of the 2000 mg L^{-1} lignin solution at pH 11.0, in which no peak corresponding to the lignin oxidation was observed. The increase in the current observed at potentials higher than 700 mV vs SCE may be related to the OER and, based on previous results, we propose that the total current (I_T) observed at this potential might have a mixed contribution, that is, $I_T = I_{O_2}(\text{OER}) + I_{\text{lignin}}$.

In the presence of ultraviolet light a significant cathodic shift of the current is observed. This behaviour has been previously observed [29] and may be explained by one of the following hypotheses: (a) in the presence of
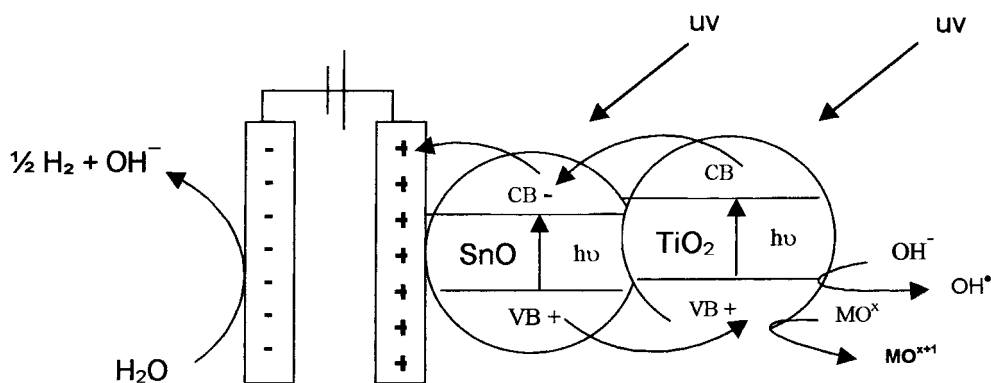

Fig. 3. Diagram illustrating the charge separation principle on a mixed oxide electrode (adapted from ref. 21). M = surface active site.
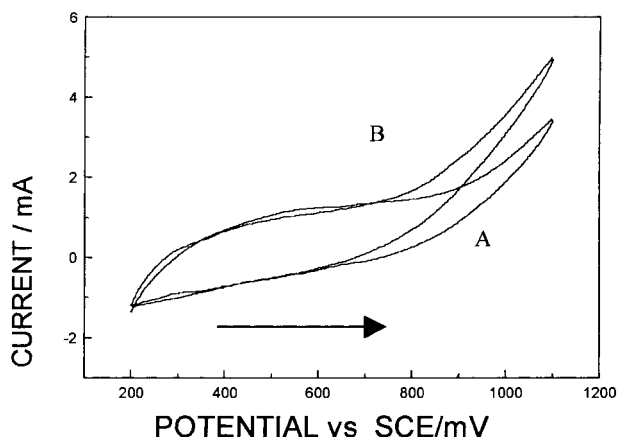
Fig. 4. Typical voltammogram of lignin solution (2000 mg L^{-1}) of Ti/Ru$_{0.1}$Sn$_{0.6}$Ti$_{0.3}$O$_2$electrode. (A) without u.v.-light, (B) in the presence of u.v.-light, pH 11, $T = 35$ °C, $v = 20$ mV s^{-1}.

high-energy photons (u.v.–light) the external bias can contribute to a decrease in the electron–hole pair recombination process; (b) the u.v.-photons reach the electrode surface during the electrochemical step and form exited radicals: $MO_X(OH^{\cdot}) + hv \rightarrow MO_X(OH^{\cdot})^{*}$, which can enhance the dye degradation, (c) photoactivation of electrochemically generated reactive species, that is, O_3 and H_2O_2, which can enhance the OH$^{\cdot}$ radical yields.

3.3. Degradation study

A complete 2^3 factorial design [30] was used to investigate the influence of experimental parameters on lignin degradation in the photoelectrochemical process. The parameters analysed were decoloration, TOC and total phenol reductions. Table 1 presents results from two experimental sets. The first set (runs 1 to 4) corresponds to the electrochemical process only, which was conducted at two different potentials (2 V (−) and 6 V (+)), while the second set (runs 5 to 8) corresponds to the combined photoelectrochemical process. For the elect-

Table 1. Experimental 2^3 factorial design to illustrate the synergistic effect between the photochemical and electrochemical process. Ti/Ru$_{0.1}$Sn$_{0.6}$Ti$_{0.3}$O$_2$ electrode. pH 11, $T = 35$ °C, $C = 2000$ mg L^{-1}

Parameter	Level (−)	Level (+)		
Potential/V	2.0	6.0		
oxygen	Without	With		
u.v. irradiation	Without	With		

Run	Potential	Oxygen	UV	Reduction/%		
				Colour	TOC	Phenols
1	−	−	−	4	0	4
2	+	−	−	4	2	9
3	−	+	−	3	0	3
4	+	+	−	19	2	10
5	−	−	+	17	5	29
6	+	−	+	70	51	82
7	−	+	+	19	6	28
8	+	+	+	72	56	80

rochemical nonirradiated process alone, the highest decoloration ratio (about 19%) was observed for 6 V between the working and the counter electrode pair. Furthermore, the other experimental parameters investigated (TOC and phenolic reduction) confirm only slight degradation using the electrochemical process alone. This result confirms earlier studies [16] which demonstrate a mild electrochemical degradation of lignin. This effect may be explained by the electrode surface becoming blocked by intermediate species arising from first electron transfer, which results in the low TOC and phenolic reduction yields observed [31].

For the coupled photochemical and electrochemical system, the degradation rates, as measured by all three parameters, are significantly higher. Yields of 72% and 80% of colour and phenolic reduction respectively, were obtained for an applied potential of 6 V. In addition a TOC reduction of more than 50% combined with 80% of phenolic reduction was observed. In order to evaluate the photoelectrochemical reduction of acute waste toxicity, the lignin solution was submitted to the Fia-E-Coli test [32] before and after the photoelectrochemical treatment. The results showed a 22% inhibition of CO_2 production for the treated solution compared with 47% for untreated solution, demonstrating that the toxicity of the waste is substantially decreased after the photoelectrochemical process (−55%).

Table 1 shows that an additional supply of oxygen (run 5 to 8), was unnecessary to achieve the reductions in the experimental parameter analysed. Furthermore, Table 2 shows that neither light nor an electric field alone results in high degradation rates. However, the slight colour increase observed for the photochemical process can be explained by formation of coloured quinonic structures. The lower photochemical activity of rutilic TiO_2 [8] may explain the low overall efficiency of the photochemical process alone. Comparing the values for the photo-electrochemical processes with the sum of the ratios obtained for the individual processes demonstrates a significant synergetic effect. When the potential was increased from 2 to 6 V, the decoloration ratio remained almost constant in the nonirradiated system (4%). However, for the photoelectrochemical system, decoloration enhancements of about 53% were observed with an increase in the potential. Similar effects were also observed in the TOC and total phenolic reduction.

3.4. Kinetic study

Kinetic studies are presented in Figure 5, which show that the colour and the total phenol content decrease

Table 2. The performance of Ti/Ru$_{0.1}$Sn$_{0.6}$Ti$_{0.3}$O$_2$ electrode over the different process tested. pH 11, $T = 35$ °C, $C = 2000$ mg L^{-1}

Reduction/%	Colour	Total phenol	TOC
Photochemical process	1	12	−5
Electrochemical process	3	9	7
Photoelectrochemical process	50	81	70
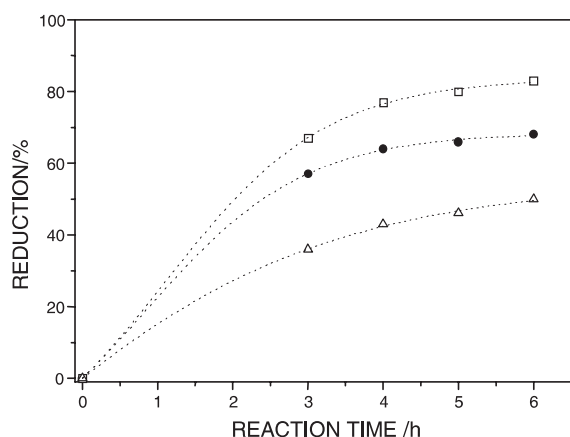
Fig. 5. Degradation yields of lignin at Ti/Ru$_{0.1}$Sn$_{0.6}$Ti$_{0.3}$O$_2$ electrode. pH 11, T = 35 °C, C = 2000 mg L^{-1}. Key: (●) colour, (□) total phenols and (△) total organic carbon.

Table 3. The effect of electrode composition on lignin degradation in the photoelectrochemical process. pH 11, T = 35 °C, C = 2000 mg L^{-1}

Electrode composition	% Reduction for the photoelectrochemical process		
	TOC	Phenols	Colour
Ti/Ru$_{0.1}$Ti$_{0.9}$O$_2$	30	50	41
Ti/Ru$_{0.1}$Sn$_{0.2}$Ti$_{0.7}$O$_2$	35	65	48
Ti/Ru$_{0.1}$Sn$_{0.6}$Ti$_{0.3}$O$_2$	70	81	50

molecules at the electrode and results in complete combustion of the organic material [20, 33, 34]. Linear correlations between the results and the SnO$_2$ content were observed for all three experimental parameters measured: decolorization ($r = 0.991$); total phenol reduction ($r = 0.995$); and total organic carbon reduction ($r = 0.982$).

rapidly at the beginning of the photoelectrochemical treatment with a reduction greater than 50% after 3 h. The lesser decrease of the total organic carbon content observed in these kinetic studies may be explained in terms of the complexity of the mineralization process. Initial lignin degradation due to cleavage at the polymer extremities may result in the formation of several phenolic derivatives (ex. catechol and vanillin). More elementary chemical compounds such as methanol, ethanol, formaldehyde, formic and oxalic acid, etc; are then generated in subsequent stages [8]. Therefore, the complete LS mineralization process involves higher order reactions.

The chemical modification of the lignin polymer during the photoelectrochemical process was monitored by gel permeation chromatography. The results indicate that after a reaction time of 6 h the lignin molecule was fragmented to a significant degree, which implies the formation of transient compounds with low molecular weight. The identification of these low molecular weight products is currently under investigation.

3.5. *Effect of electrode composition*

To evaluate the relationship between the SnO$_2$ content of the modified electrode and the efficiency of the photoelectrochemical process, three different electrode compositions were evaluated: Ti/Ru$_{0.1}$Ti$_{0.9}$O$_2$; Ti/Ru$_{0.1}$Sn$_{0.2}$Ti$_{0.7}$O$_2$ and Ti/Ru$_{0.1}$Sn$_{0.6}$Ti$_{0.3}$O$_2$.

Two factors explain the efficiency of the SnO$_2$ electrodes which is shown in Table 3. (i) The introduction of a second semiconductor (SnO$_2$) improves the charge separation process which increases the photochemical efficiency of the whole process [21]. As previously mentioned, one of the limiting factors in a photochemical process is the inactivation of the photocatalyst by recombination of the photogenerated electrons with their associated holes. (ii) Coatings containing a higher ratio of SnO$_2$ favour hydroxyl radical (OH$^•$) formation, which reacts with organic

4. Conclusion

The results obtained demonstrate that the efficiency of the electrochemical degradation of lignin can be significantly improved by applying a simultaneous photoelectrochemical process. This combined process permits high decoloration and total phenolic reduction ratios (higher than 50% for a reaction time of 3 h) and mineralization of about 30%, in a 2000 mg L^{-1} LS aqueous solution. The high efficiency of the electrode coatings tested in the photoelectrochemical process may be explained as follows:

(i) In the presence of UV light ($\lambda = 254$ nm) the external potential applied contributes to reduce the electron–hole pair recombination process of the semiconductor species (E_g, bandgap energy, for SnO$_2$ = 3.8 eV and E_g for TiO$_2$ = 3.2 eV [35]) (Figure 3).

(ii) Since the process is conducted in an undivided cell, the photoactivation of relatively long lifetime species formed at the electrode surface, that is, H$_2$O$_2$ (formed on the cathode side) [36] and O$_3$ (formed on the anode side) [37], contribute to enhance the degradative capacity of the process. This enhancement is related to the powerful oxidant character of these transient species, and to the enhanced formation of hydroxyl radicals according to the following reaction sequence [38]:

$$O_3 + H_2O + h\nu \rightarrow H_2O_2 + O_2$$
$$H_2O_2 + h\nu \rightarrow 2\,OH^•$$
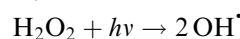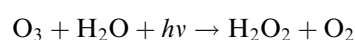
Preliminary results suggest that the use of a Ti/Ru$_{0.1}$Sn$_x$Ti$_{(0.9-x)}$O$_2$ electrode in a photoelectrochemical process may be a promising alternative for treatment of wastes with a high content of recalcitrant lignin derivatives. We are currently constructing a reactor in order to evaluate an efficient long-term photoelectrochemical degradation process for organic waste compounds.

References

1. R. Dong and S. Wu, *Wat. Res.* **30** (1996) 577.
2. L. Chapaoux, *Environ. Pol.* **92** (1996) 147.
3. T. Xie, K. Abrahamsson, E. Fogelqvist and B. Josefsson, *Environ. Sci. Technol.* **20** (1986) 457.
4. S. Odendahl, *Pulp & Paper Canada* **95** (1994) 30.
5. H. Palm and R. Lammi, *Environ. Sci. Technol.* **29** (1995) 1722.
6. J. Sundquist, *Paperi Ja Puu – Paper and Timber* **76** (1994) 22.
7. A.L. Linsebigler, L. Guangquan and T. Yates Jr., *J. Chem. Rev.* **95** (1995) 735.
8. M.R. Hoffmann, W. Choi and D.W. Behnemenn, *Chem. Ver.* **95** (1995) 69.
9. P. Peralta-Zamora, S.G. Moraes, R. Pelegrini, M. Freire Jr., J. Reyes, H. Mansilla and N. Durán, *Chemospere* **36** (1998) 2119.
10. G. Riegel and J.R. Bolton, *J. Phys. Chem.* **99** (1995) 4215.
11. J. Zhao, T. Wu, K. Wu, K. Oidawa, H. Hidaka and N. Serpone, *Environ. Sci. Technol.* **32** (1998) 2394.
12. P. Peralta-Zamora, E. Esposito, R. Pelegrini, R. Groto, J. Reyes and N. Durán, *Environ. Technol.* **19** (1998) 55.
13. K. Rajeshwar, J.G. Ibanez and G.M. Swain, *J. Appl. Electrochem.* **24** (1994) 1077.
14. A. Savall, *Chimia* **49** (1997) 23.
15. C. Chiang, J.E. Chang and T.C. Wen, *Wat. Res.* **29** (1995) 71.
16. C. Li-Choung, J-En Chang and S-Chuan Tseng, *Water Sci. Technol.* **36** (1997) 123.
17. A. Fujishima and K. Honda, *Nature* **238** (1972) 37.
18. C.C. Sun and T.C. Chou, *Ind. & Eng. Chem. Research.* **37** (1998) 4207.
19. M. Kesselman, N.S. Lewis and M.R. Hoffmann, *Environ. Sci. Technol.* **31** (1997) 2298.
20. O. Simond, V. Schaller and Ch. Comninellis, *Electrochim. Acta* **42** (1997) 2009.
21. K. Vinodgopal, S. Hotchandani and P.V. Kamat. *J. Phys. Chem.* **97** (1993) 9040.
22. J.F.C. Boodts and S. Trasatti, *J. Electrochem. Soc.* **137** (1990) 3784.
23. L.L. Houk, S.K. Johnson, J. Feng, R.S. Houk and D.C. Johnson *J. Appl. Electrochem.* **28** (1998) 1167.
24. L.D. Burke and J.F. Healy, *J. Electroanal. Chem.* **124** (1981) 327.
25. D.T. Shieh and B.J. Hwang, *Electrochim. Acta* **38** (1993) 2239.
26. R.I. Beckley, T.G. Carreno, J.S. Lees, L. Palmisano and R.J. Tilley, *J. Solid State Chem.* **92** (1991) 178.
27. L. Lipp and D. Pletcher, *Electrochim. Acta* **42** (1997) 1091.
28. S-M. Lin and T.C. Wen, *J. Appl. Electrochem.* **23** (1993) 487.
29. R. Pelegrini, P. Peralta-Zamora, A.R. de Andrade, J. Reyes and N. Durán, *Appl. Catal. B: Environ.* **22** (1999) 83.
30. R.F. Rocha, S.S. Rosatto, R.E. Bruns and L.T. Kubota, *J. Electroanal. Chem.* **433** (1997) 73.
31. A.R. de Andrade, P.M. Donate, P.A. Alves, C.H.V. de Fidellis and J.F.C. Boodts, *J. Electrochem. Soc.* **145** (1998).
32. W.F. Jardim, C. Pasquini, J.R. Guimarães and L.C. Faria, *Water Res.* **24** (1989) 351.
33. Ch. Comninellis and G.P. Vereesi, *J. Appl. Electrochem.* **21** (1991) 335.
34. Ch. Comninellis and A. De Battisti, *J. Chim. Phys. Phys.-Chim. Biol.* **93** (1996) 673.
35. K. Vindogopal and P.V. Kamat, *Environ. Sci. Technol.* **29** (1995) 841.
36. D. Pletcher and C. Ponce De Leon, *J. Appl. Electrochem.* **25** (1995) 307.
37. A.G. Vlyssides and C.J. Israilides, *Environ. Poll.* **97** (1–2) (1997) 147.
38. R. Freshour, S. Mawhinney and D. Bhattacharyya, *Wat. Res.* **30** (1996) 1949.